



The Society shall not be responsible for statements or opinions advanced in papers or discussion at meetings of the Society or of its Divisions or Sections, or printed in its publications. Discussion is printed only if the paper is published in an ASME Journal. Authorization to photocopy material for internal or personal use under circumstance not falling within the fair use provisions of the Copyright Act is granted by ASME to libraries and other users registered with the Copyright Clearance Center (CCC) Transactional Reporting Service provided that the base fee of \$0.30 per page is paid directly to the CCC, 27 Congress Street, Salem MA 01970. Requests for special permission or bulk reproduction should be addressed to the ASME Technical Publishing Department.

Copyright © 1997 by ASME

All Rights Reserved

Printed in U.S.A.

SOOT PREDICTIONS WITHIN AN AERO GAS TURBINE COMBUSTION CHAMBER

H. T. Brocklehurst, C. H. Priddin

ROLLS-ROYCE plc,
PO Box 31
Derby DE24 8BJ
U.K.

J. B. Moss

Cranfield University,
Cranfield,
Bedford MK43 0AL
U.K.



ABSTRACT

This paper presents two different soot production models and their predictions in a practical combustion chamber. These predictions are compared with detailed internal measurements of soot concentration by probe sampling. Both models solve two additional transport equations for soot mass concentration and number density, and incorporate representations of source terms for particle nucleation, surface growth, coagulation and oxidation. In one approach these rates are inferred from soot property measurements in a confined turbulent jet flame, and in the other from a flamelet-based approach employing computations of a kerosene laminar counter-flow flame which incorporates detailed reaction kinetics. Preliminary results from both models are encouraging. Although both over predict the peak levels of soot measured in a gas turbine combustor at 7 bar, these computations have neglected the effects of radiation, which will be included in subsequent calculations. The approach based on detailed chemistry captures more accurately the very high rate of oxidation towards the combustor exit which is a pronounced feature of the measurements and is missing in earlier reported studies. This is related to differences in the coagulation model. Calibration of model parameters for the empirical model from simple experiments leads to exaggerated coagulation at the higher combustor temperatures, reduced soot number densities and under-estimates effective surface area for oxidation. The suitability of laminar flamelet counter-flow flames as a route to generating the soot production relationships necessary for combustor predictions are carefully reviewed in the light of strain rate and residence time effects on detailed hydrocarbon pyrolysis.

INTRODUCTION

Computationally-based modelling of soot formation and oxidation within gas turbine combustors remains challenging as the detailed processes are poorly understood and computational constraints are such that complex models cannot be included. This area is of great practical importance in the development of combustion chambers, not only because of the necessity of complying with emissions legislation, but also because substantial soot production within the combustor will have a significant effect on metal temperatures. Large quantities of soot will lead to increased heat transfer to the walls by radiation, which in turn will have an impact on combustor lifetime. Also, the production of thermal (Zeldovich) NO_x and other pollutants is very dependent on local temperature and hence the

reduction due to radiation from soot particles will have a significant impact on the amounts produced.

Several approaches have been adopted to model the soot formation and consumption process in turbulent flows. Magnussen et al. (1978) incorporated the soot model first proposed by Tesner et al (1971) within the framework of their Eddy Dissipation Combustion Model. However, the interaction with flow turbulence is not represented and the combustion description means the approach cannot be easily extended to different fuels or operating conditions. Other approaches rely on developments of the laminar flamelet concept, which assumes that turbulent reacting flow consists of a collection of reaction diffusion layers which are continuously displaced and stretched by the turbulence. The layers are assumed to be one-dimensional and similar in structure to one-dimensional counter-flow laminar flames. These are transported and distorted by the flow, but retain the same identifiable structure and can therefore be reduced to dependence on a single scalar variable, the mixture fraction for non-premixed flames. In the simplest applications the relationships between the mixture fraction and other composition variables can be derived either from measurements in laminar flames or from laminar flamelet calculations, including detailed chemistry. Gore and Faeth (1986) extended this approach to develop an empirical relationship between the soot volume fraction and the mixture fraction. However, this neglects the fact that the time scales of the soot formation processes are long compared to mixing, resulting in soot being a function of both mixture fraction and residence time. In tackling a similar problem, Bilger (1976) postulated that although soot itself should not be described by a single relationship with mixture fraction, its volumetric source term may. This relies on the assumption that quantities of soot produced are small enough to be considered as a perturbation to the laminar flamelet. This approach has also been applied to the prediction of NO_x with some success. The formation and oxidation of soot are thus related to the local mixture fraction, either by using empirical models based on laminar flamelet measurements (Moss et al. (1988)) or through the inclusion of these processes in detailed calculations of a laminar flamelet including detailed reaction kinetics (Leung et al. (1991)). The results achieved using the former approach give good agreement with measurements close to the conditions at which the model was calibrated. However, laboratory experiments are invariably far from engine operating conditions. The second approach is more fundamentally based, and allows the inclusion of more detailed information about the fuel breakdown path and the influence of pyrolysis products, such as

acetylene and benzene, on the soot formation process. The issues of calibration are therefore avoided.

Both of these models have been demonstrated within simplified geometries, but they require further validation within the more complex flows encountered in a gas turbine combustor before they can be used with confidence for design calculations. This paper describes the application of these models to predict the flows within a four sector annular combustor. This geometry was selected as internal measurements of soot and other species concentrations have been carried out by the Defence Research Agency (DRA) Pyestock at an inlet pressure of 6.65 bar and inlet temperature of 850 K (Hurley 1993). Though the operating conditions are not representative of full power conditions, the inlet temperatures are typical and this will offer a discriminating test of the abilities of these models.

NUMERICAL SIMULATION

The calculations of the combustor were carried out with the Rolls-Royce CFD code, PACE, which has been widely applied to the prediction of the fully turbulent flow in gas turbine combustion systems (Priddin and Coupland, 1988, and Coupland et al., 1991). Only a brief summary of key features of the code will be given; see references given above for more detail.

PACE uses a two-dimensional orthogonal mesh rotated to form a three-dimensional grid, which allows a fair degree of flexibility in the geometries that can be studied. The standard $k-\epsilon$ model is used in conjunction with the pressure correction method SIMPLE. A variety of differencing schemes are available, but in this calculation Hybrid Linear Parabolic Algorithm, HLP (Jones, 1995) was used. At the high inlet temperature and pressure conditions typical of gas turbine operation, combustion chemical kinetics are very fast compared to the mixing timescales. In the limit of fast chemistry the molecular species may be instantaneously related to the mixture fraction, f . To model the effects of turbulent interaction on the mean values, an additional transport equation for the mixture fraction variance is solved and a beta function assumed for the probability density function. The relationships between the thermochemical variables of interest and the mixture fraction are derived from a laminar flamelet calculation (Leung 1996).

SOOT FORMATION

A cloud of soot particles may be characterised by the total mass of soot, expressed in terms of soot mass fraction c_m and the number density of the particles N (particles/kg of mixture). However, given the strong time dependence of soot formation on residence time, it is not possible to derive direct relationships between these variables and mixture fraction. Rather the volumetric source terms for nucleation, surface growth, coagulation and oxidation are related to the mixture fraction and additional transport equations for soot mass fraction and number density terms are solved. Within PACE the source terms are given by

$$\bar{\rho} \frac{d}{dt} (\bar{N}) = \bar{\rho} \bar{R}_{NU} - \bar{\rho} \bar{R}_{CO} \bar{N}^2 \quad 1$$

$$\bar{\rho} \frac{d}{dt} (\bar{c}_m) = \bar{\rho} \bar{R}_{SG} \bar{N} + \bar{\rho} C_s \bar{R}_{NU} - \bar{\rho} \bar{R}_{OX} \bar{c}_m \quad 2$$

where \bar{R}_{NU} is the Favre averaged nucleation rate (particles/kg/s), \bar{R}_{CO} is the coagulation rate (kg/s/particle), \bar{R}_{SG} is the surface growth rate (kg/s/particle) and \bar{R}_{OX} is the Favre averaged oxidation rate. C_s (kg/particle) is a constant representing the mass of a

nucleating particle and is dependent on the soot production model used. Note that in deriving the time averaged form of the equations all cross-correlation terms have been ignored. Such a decision is unavoidable given the difficulties that would be involved in deriving suitable models for all the correlations required. The rates given by each of the two models being examined are described below.

'MOSS' SOOT PRODUCTION MODEL

The model proposed by Moss et al. (1988) is based on an empirical route for deriving the soot nucleation, surface growth and coagulation rates. The model constants have been determined from comparing experimental measurements in laminar and turbulent jet flames up to pressure of 7 bar with predictions. The activation temperatures (T_α and T_γ) are taken directly from Gilyazetdinov (1972).

The source terms are expressed as

$$\begin{aligned} R_{NU} &= C_\alpha N_0 \rho T^{1/2} [X_C] e^{-T_\alpha/T} \\ R_{CO} &= \frac{C_\beta}{N_0} T^{1/2} \rho \\ R_{SG} &= C_\gamma \rho T^{1/2} [X_C] e^{-T_\gamma/T} \end{aligned} \quad 3$$

where the model constants have been assigned the values

$$\begin{aligned} C_\alpha &= 1.7 \times 10^8 \quad (1/m^3s) & T_\alpha &= 46100 \\ C_\beta &= 9 \times 10^{19} \quad (m^3/s) \\ C_\gamma &= 1.26 \times 10^{-11} \quad (kg/s) & T_\gamma &= 12600 \\ C_\delta &= 144 \quad (kg/particle) \end{aligned}$$

In addition, N_0 is Avogadro's number and $[X_C]$ is the mole fraction of a soot precursor. This model is the same as that used by Alizadeh and Moss (1993) to compute a tubular combustor, with constants derived for ethylene, following the approach of Young et al. (1991). The calculations of Alizadeh and Moss assumed that the soot precursor was the sum of the unburnt hydrocarbons, whereas the work of Young et al. assumed it to be simply the parent fuel. In the present work it has been taken to be the sum of the acetylene and benzene mass fractions, given that the benzene content of the fuel is likely to be a key factor in the quantities of soot produced. The relationships of these rates with mixture fraction were calculated using the results of the counter-flow laminar flamelet code described below, though no soot species were included in the calculation.

'LINDSTEDT' SOOT PRODUCTION MODEL

The counter-flow laminar flamelet model developed by Leung (1996) and Leung et al. (1991) and used in this study models the flow and detailed combustion chemistry in a laminar counter-flow flame. The fuel emanates from a porous cylinder into an opposing air stream, illustrated in figure 1. A stable reaction zone is established on the weak side of the stagnation point, and fuel and oxidant diffuse towards the reaction zone with an imposed velocity gradient. There is strong coupling between the fluid mechanics (fuel-air mixing rates) and the chemical kinetics (reaction rates) leading to reaction zone structures that are strong functions of velocity gradient. Within this simple flow field, detailed chemical kinetics are solved using a kinetic scheme including 460 reactions and 80 species. Soot is modelled by calculating the soot number density and the mass fraction of carbon in soot. The sources for each of these variables again include simplified representations of the processes of nucleation, surface growth, coagulation and oxidation.

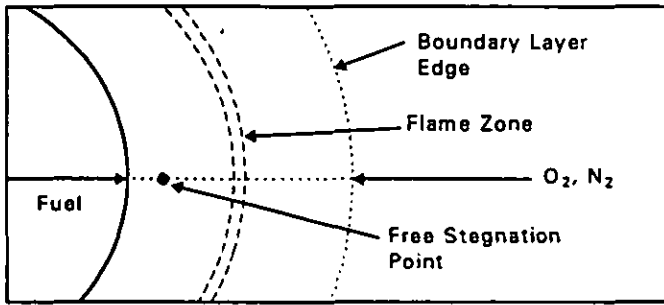
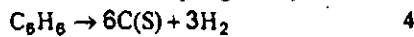


Figure 1 Counter-Flow Flamelet Geometry

Nucleation is modelled by assuming that the formation of soot is dependent on the presence of (poly-) aromatic rings, originating either from the pyrolysis of the fuel or from the parent fuel. The second route is particularly important for fuels with a high aromatic content, such as kerosene. The nucleation step is given by



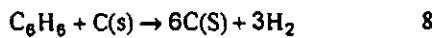
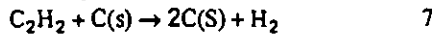
where $C(S)$ is the carbon contained in the soot particles. The reaction step is approximated by assuming that the particles formed contain a certain minimum number of carbon atoms. This assumption results in a source term for the number density of

$$R_{NU} = k_{nucl} [C_6H_6] \frac{MW}{\rho C_6} \quad 5$$

where MW is the mixture molecular weight and C_6 is 720 for an assumed C-60 shell, which gives an initial particle size of 1 nm. The reaction rate constant k_{nucl} is then given by

$$k_{nucl} = 0.75 \times 10^5 e^{-171544/RT} \quad 6$$

Acetylene is taken as the adsorbed species responsible for soot mass growth at high temperatures. In more complex fuels, particularly those already containing some aromatics, there will be an additional path for surface growth due to the presence of benzene. The reaction steps can be written schematically as



with the reaction rates given by

$$r_{sg1} = k_{sg1} \frac{MW_c}{\rho} [C_2H_2] \quad 9$$

$$r_{sg2} = k_{sg2} \frac{MW_c}{\rho} [C_6H_6] \quad 10$$

where MW_c is the molecular weight of soot (12.011 kg/kmol). This assumes that the surface growth is linearly dependent on number density and independent of surface area. The rate constants are assumed to be identical and are given by

$$k_{sg1,2} = 0.11 \times 10^{-11} e^{-100764/RT} \quad 11$$

The total surface growth rate is given by the sum of these two rates, i.e.

$$R_{SG} = r_{sg1} + r_{sg2} \quad 12$$

The decrease of soot particles due to coagulation is modelled using the normal square dependence inferred from kinetic theory (Fuchs 1962), given by

the percentage conversion of soot might also be expected to be much lower, and the perturbation to the local chemistry due to soot could

$$R_{CO} = -2C_a \left(\frac{6k_B T}{\rho C(s)} \right)^{1/2} \quad 13$$

where C_a is the agglomeration constant ($= 9$) and k_B the Boltzman constant ($1.38e-23$ J/K). The model also includes a dependence on the square root of the soot particle density, which requires a modification to equation 1.

The fuel used in these calculations is pseudo kerosene, which is taken here to be gaseous and a mixture of 80% C11H24 and 20% C6H6 by volume.

SOOT OXIDATION

Both of the models described above were derived in diffusion flame geometries in which the oxidation and formation regions are largely separate, and therefore the respective rates of these processes are in principle independent. The same oxidation model, that of Nagle and Strickland-Constable (1962), has been adopted in conjunction with both formation models.

APPLICABILITY OF OPPOSED JET LAMINAR FLAMELET FOR TURBULENT CALCULATIONS

The counter-flow flame used in the Lindstedt model features a stagnation point (figure 1), at which the residence time becomes very large. This is particularly significant for non-diffusing species, such as soot. As a result of the direct dependence of soot produced on residence time, the peak soot produced in these flames occurs in the neighbourhood of the stagnation point, where the mixture is rich and the temperature relatively low. The results for a flame at 6.65 bar and an inlet air temperature of 850 K (figure 2), show the peak soot volume fraction occurring at a mixture fraction of 0.58 and temperature of 1161 K, conditions which are not realised in the gas turbine combustor. 1161 K is a very low temperature for the formation of soot, as Glassman et al. (1994) have found that the lowest temperature at which soot particle inception occurs is about 1450K. In contrast, the peak number density occurs at a mixture fraction of 0.16, where the temperature is much higher (1838 K). A similar effect has been reported by Sivathanu et al. (1994) who state that the nucleation of soot takes place in the high temperature regions closer to the stoichiometric mixture fraction, while surface growth takes place at richer concentrations, even when the temperature is comparatively low.

There are concerns that the unrepresentative soot volume fraction profile could affect the inferred soot production rates, which would then imply that they cannot be used to predict soot in full combustor calculations. To assess the size of this effect, the production rates were monitored as time elapsed (figure 3). There is little change in the soot production rates, in spite of large increases in the soot volume fraction. This is because the nucleation rates are independent of the existing soot levels and surface growth rates are not dependent on the surface area of the soot particles, but the number density. After an initial adjustment, the number density is insensitive to elapsed time and hence the rates converge, thus removing the concerns over the use of the predicted rates in a full combustor calculation.

Despite the high residence times of 0.01s at the stagnation point, only 6% of the local carbon is converted to soot. As the residence time in a gas turbine combustion chamber is much lower (~ 5 ms) thus be negligible. This suggests that the approach outlined above for soot modelling should be valid for a gas turbine combustor.

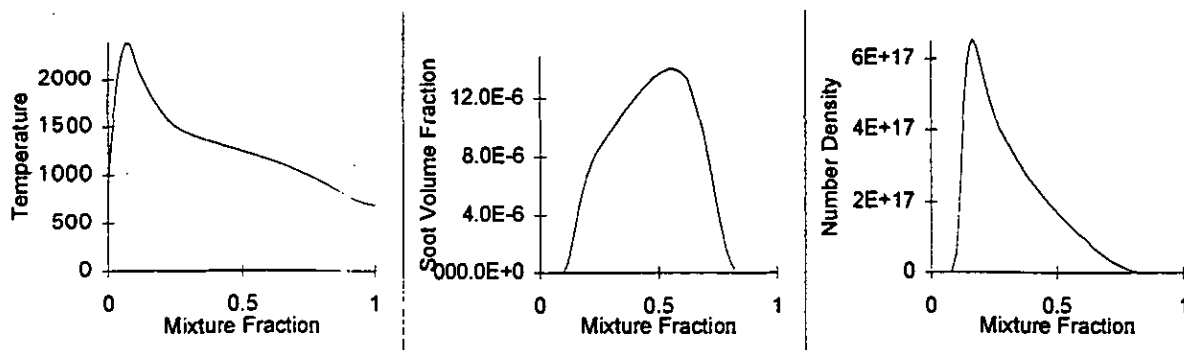


Figure 2 Results from Counter-Flow Laminar Flamelet Code at 6.65 bar and Strain of 1000 s^{-1}

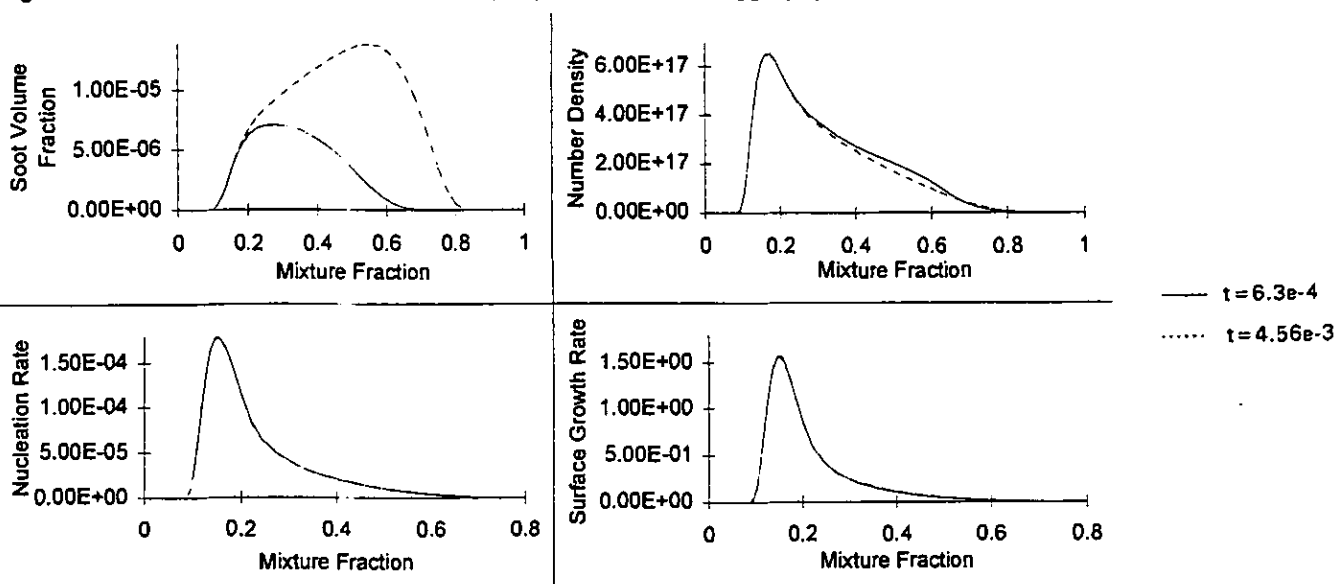


Figure 3 Changes in Soot Volume Fraction, Number Density and Production Rates with Elapsed Time

In addition to this peculiarity of the geometry, the counter-flow flame is strained and the predictions are dependent on the strain rate. Figure 4 indicates that higher strain rates lead to increased surface growth and nucleation rates. This is due to the reduced residence time at the higher strain rates, leading to benzene penetrating further towards weaker mixture fractions and hence higher temperatures. This indicates that careful selection of the strain rate is necessary for a full combustor calculation.

COMBUSTOR CALCULATIONS

These models were both applied to an RB211 phase 2 combustor in which measurements of species, temperature and soot have been carried out by DRA at three internal planes and the exit plane (Hurley, 1993). The measurement campaign covered four sectors, with measurements being carried out over the central two sectors to minimise the effects of the side walls. Measurements are reported at an inlet pressure of 6.65 bar and inlet temperature of 850 K. Although a gas turbine combustor operates at 40 bar at take-off, all other conditions have been matched. This geometry provides a good test of the soot models described previously, but does not test whether or not they are capable of being extended to higher pressure conditions, where the quantities of soot produced are likely to be extreme.

Only one sector of the flametube was modelled, with cyclic symmetry applied to the boundaries. Flow splits were derived from a one-dimensional empirical calculation, and were verified through comparison of the measured and predicted mixture fraction (see figure 5). It was found necessary to reduce the turbulent Prandtl number for the mixture fraction to 0.4 to enhance the scalar mixing. It is thought that this low turbulent Prandtl number is needed since the $k-\epsilon$ model is not capable of accurately modelling the highly swirling flows found in the Primary Zone of this combustor. This deficiency may be addressed by a fully combusting Reynolds-Stress model. Radiation from the soot was not modelled, despite indications (c.f. Sivathanu et al. (1994)) that the heat loss from heavily sooting flames, such as may be found in combustion chambers, is likely to be large. The magnitude of this effect has been studied within the counter flow laminar flamelet geometry, where radiation from the soot was modelled using the optically thin approximation. i.e. each cell of the flame would radiate to the surroundings with no interchange with other regions of the flame. The loss of energy from the flame was determined from

$$Q_{\text{emitted}} = C_0 f_v T^S$$

where Q_{emitted} is the enthalpy loss due to radiation, C_0 is a constant equal to $2.77 \times 10^{-7} \text{ kW/m}^3/\text{K}^5$, T is the temperature and f_v is the local soot volume fraction. This equation is taken from Gore and Jang

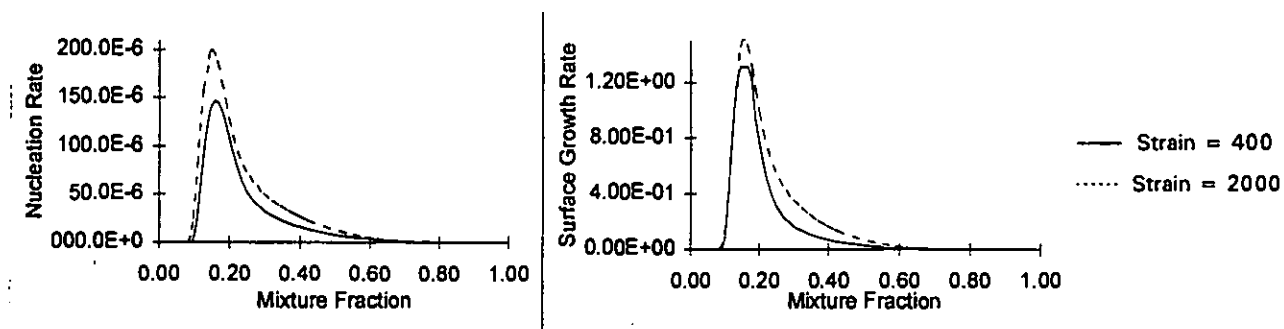


Figure 4 Effect of Strain on Predictions of Counter-Flow Laminar Flamelet at 6.65 Bar and Strain of 1000 s^{-1}

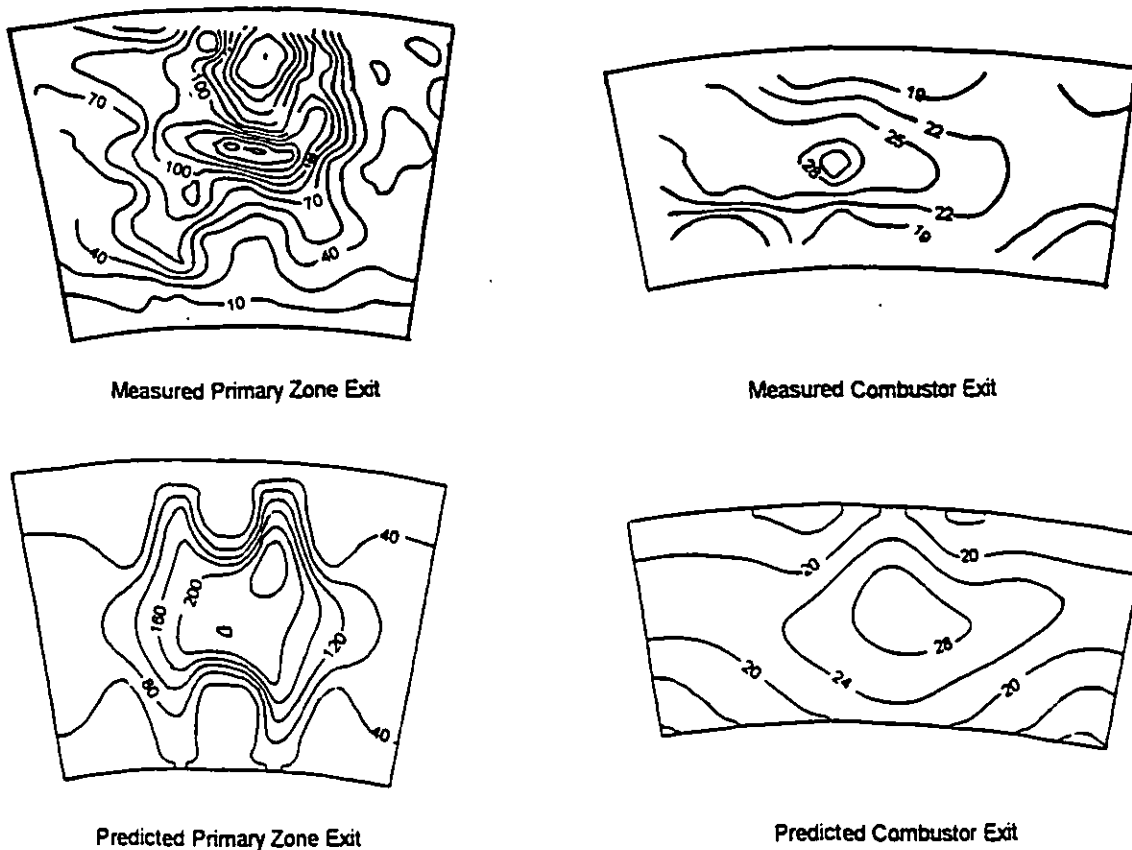


Figure 5 Comparison of Measured and Predicted Soot in Gas Turbine Combustor (mg/m^3)

(1992). Including this term reduces flame temperature in a manner which is not confined to the regions of high soot mass fraction. The peak flame temperature is reduced by 200 K. As a result the peak soot volume fraction is reduced by a factor of about 2.5.

As highlighted above, the production rates predicted by the Lindstedt detailed chemistry model are directly affected by the strain rate of the flame. Since it would be complex and expensive to use the local strain rate given by the CFD calculation to select the most appropriate laminar flamelet, it was decided to select a single laminar flamelet on the basis of the mean strain rate in the calculation. The strain rate was derived from the values of k and ϵ given by the flow

field calculation; this strain rate based on the turbulence length scales is arguably more relevant than the mean strain rate since combustion occurs at the smallest length scales. The mean was calculated by using values only in regions where the mixture fraction lay between 0.06 and 0.2 where soot production is significant; higher strain rates can be found in regions where the mixture strength is unfavourable for soot production such as in the shear layer of the fuel injector. A strain rate of 1000 s^{-1} was used.

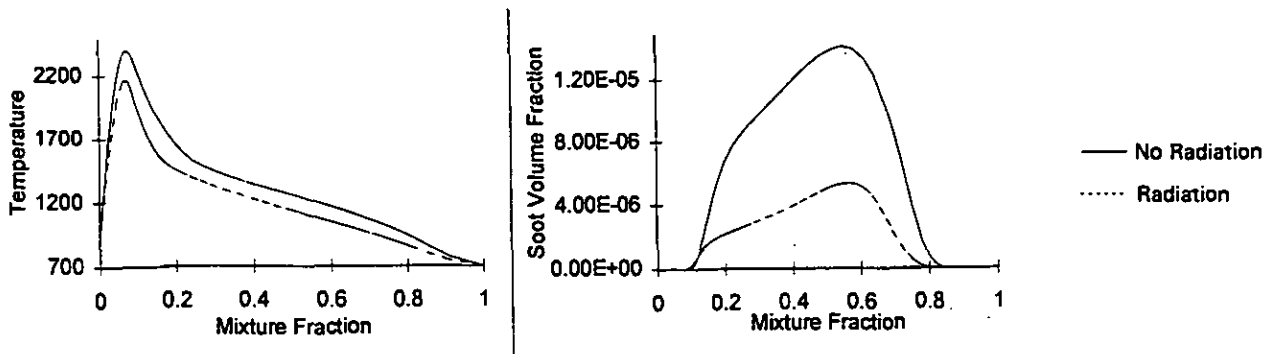


Figure 6 Effect of Radiation on Predictions of Counter-Flow Laminar Flamelet at 6.65 Bar and a Strain of 1000 s^{-1}

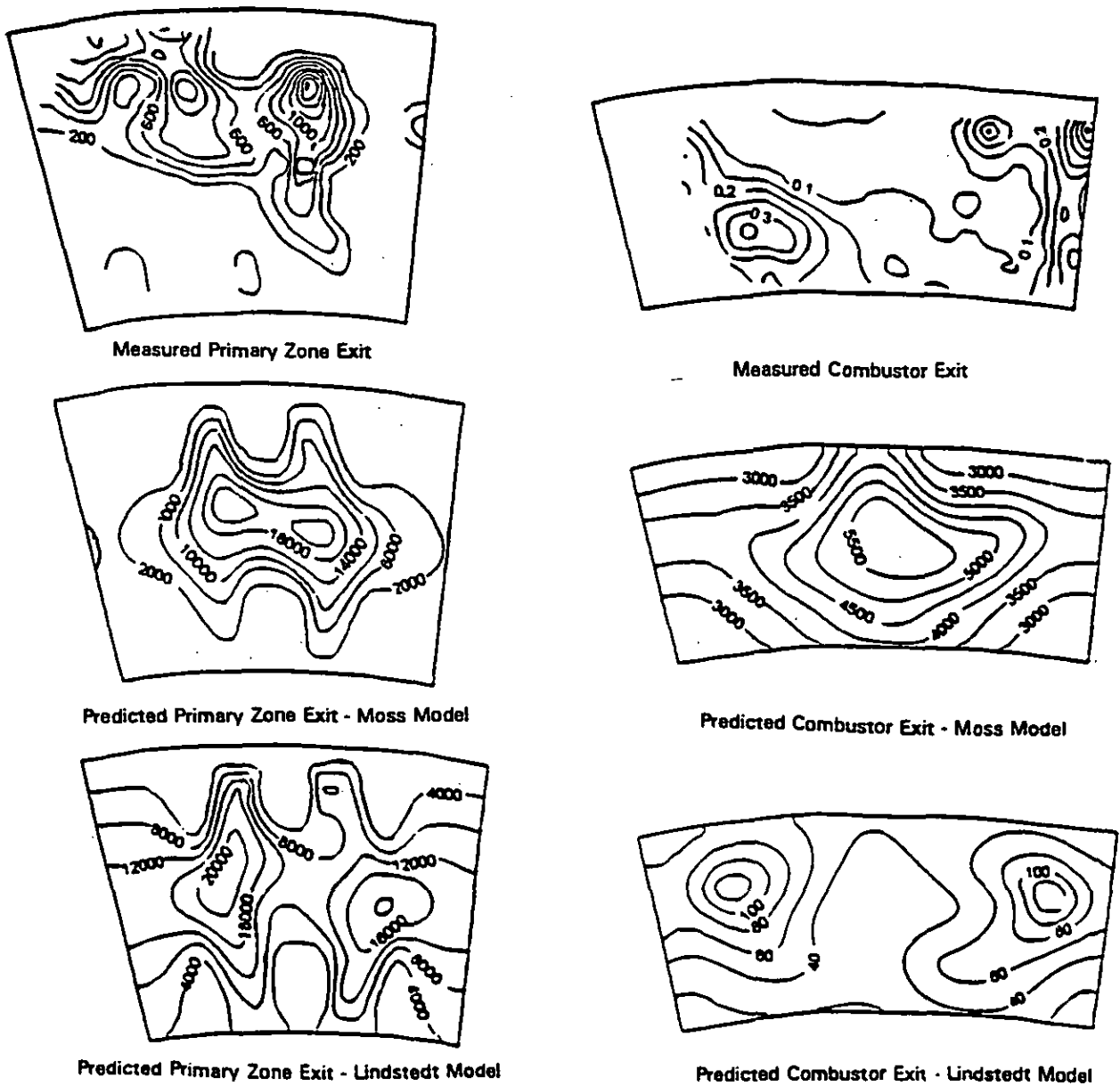


Figure 7 Comparison of Measured and Predicted Soot in Gas Turbine Combustor

RESULTS

Figure 7 shows the soot mass concentrations for the measurements and the two predictions. It is immediately obvious that there is little similarity between the pattern of the predictions and the measurements. Because of the dependence of the soot models on mixture fraction, both the predictions closely resemble the mixture fraction contour plot (figure 5), whereas the measurements of soot mass fraction and mixture fraction bear little resemblance to each other. This difference is difficult to resolve at this stage. The peak values of soot mass fraction for the predictions are very similar to each other and both are an order of magnitude higher than the measurements. This is thought to be due to neglecting the effects of radiation within the model, which given the large soot concentrations measured, will have a significant effect on the local temperature and hence the soot production rates. The magnitude of the effect of radiation has been illustrated by using the soot production rates inferred from the Lindstedt kinetic model, including the loss due to radiation. Though this calculation does not rigorously model the interaction of soot and radiation in the combustor environment, it does demonstrate the magnitude of the radiation effects. In particular the peak soot levels are now reduced to values comparable to the measurements (figure 8). This clearly demonstrates the need to closely couple the soot models with an appropriate radiation model.

Another key feature of the measurements is the rapid oxidation of the soot towards the exit of the combustor, with peak levels reducing by four orders of magnitude. Soot oxidation is directly dependent on the surface area of the soot aerosol and therefore very sensitive to the number density predicted by each model. The empirical model parameters proposed by Young et al (1991) do not capture the rapid oxidation, as the peak soot mass fraction reduces by only a factor of 4, whereas the Lindstedt model more closely matches the measurements. The key to understanding this observation is in the implied particle size or, for comparable mass concentrations, the particle number density. Figure 9 shows the number density predicted by each model, which for the Lindstedt model is 3 orders of magnitude larger than that for the Moss model, thus explaining the improved agreement of the Lindstedt model. The influence of number density has been verified by fixing the soot number density used by the Moss soot model, whilst maintaining the net production rates (R_{SGN}), resulting in a similar burn out rate to the other model.

Young et al. (1991) sought to generate particles having diameters ≥ 200 nm, consistent with their jet flame measurements, whilst indications are that primary particle size is ≤ 50 nm and, even if agglomerated to larger size, this is more appropriate for oxidation models. This accounts for the difference in the two models, and further experiments to confirm this interpretation are underway. The complex and highly turbulent flows in the combustor are such that the production and oxidation regimes overlap significantly, unlike in simple laboratory flames. This highlights the need to establish a coagulation rate that models the evolution of the soot number density correctly.

CONCLUSIONS

A methodology, based upon detailed computations of laminar kerosene-air flames burning at elevated temperature and pressure, has been demonstrated in application to soot production in a practical gas turbine combustor. Soot production rates may be inferred from these calculations although aspects of the laminar counter flow geometry are unrepresentative of the practical situation.

In a counter-flow laminar flame the maximum residence time occurs at the stagnation point, which is located at mixture fractions about 0.6. As a result the peak soot volume fraction occurs at the very rich mixture fractions in the vicinity of the stagnation point. The occurrence of the peak soot volume fractions at these rich mixtures has no effect on the soot production rates, since the nucleation rate is independent of soot concentration, and the surface growth rates are dependent on the number density only, which is unaffected by residence time.

Increasing the strain rate reduces the volume fractions of soot produced due to the reduced residence time. In contrast, an increased strain rate leads to a significant increase in the production rates due to the increased penetration of the soot precursor, benzene.

Both the models examined here over predict the levels of soot produced within a gas turbine combustor, which is believed to be due to neglecting the effects of radiation within these calculations.

The correct prediction of the oxidation rate is dependent on the accurate prediction of the surface area of the soot aerosol and hence the number density. To achieve accurate predictions, the coagulation rate used by the soot model must be capable of correctly predicting the evolution of number density along the combustor.

ACKNOWLEDGEMENTS

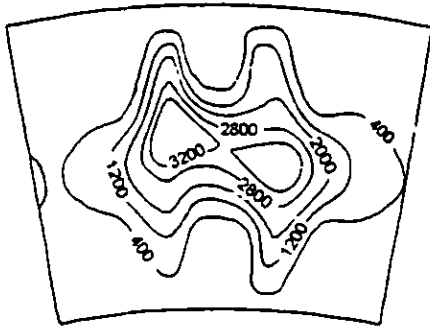
This work could not have been completed without access to the DRA measurements and their continued interest in the calculations. The authors would like to thank P. Lindstedt and K. Leung for supplying the laminar flamelet code and providing support and suggestions in its use.

REFERENCES

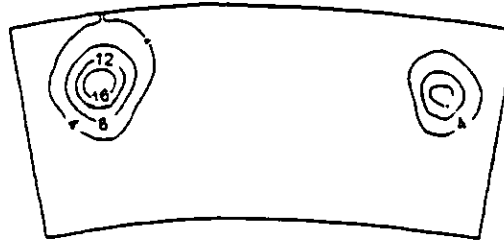
- Alizadeh, S. and Moss, J. B (1993) 'Flowfield Prediction of NOx and Smoke Production in AGARD CP536, p7:1-7:20
- Bilger, R. W. (1976), 'Turbulent Jet Diffusion Flames' Prog. Energy Combust. Sci., 1976, Vol 1, pp 87-109
- Coupland, J., Fry, P., and King, R. A., 1991, 'Application of 3-D CFD techniques to gas turbine metal temperature predictions', Tenth International Symposium on Air Breathing Engines, Nottingham, U. K., 2 - 6 September 1991.
- Fuchs, N. A. (1964) *The Mechanics of Aerosols*, Bergammon
- Gilyazetdinov, L. P. (1972) *Khim. Tverd. Topl.*, Vol. 3, pp 103-111
- Glassman, I., Nishida, O. and Sidebotham, G. (1994), 'Critical Temperatures of Soot Formation', in 'Soot Formation in Combustion: Mechanisms and Models', H. Bockhorn (Ed.)
- Gore, J. P. and Faeth, G. M. (1986) 21st Symposium (International) on Combustion, pp 1521
- Gore, J. P. and Jang, J. H., (1992) *Journal of Heat Transfer*, Transaction of ASME, 234, Vol 114, February
- Hurley, C. D. (1993), AIAA 29th Joint Propulsion Conference
- Jones, W. P., (1995), "Turbulence Modelling and Numerical Solution Methods for Variable Density and Combusting Flows", in *Turbulent Reacting Flows*, Academic Press, Libby and Williams
- Leung, K.M, Lindstedt, R.P. and Jones W. P., (1991), 'A Simplified Reaction Mechanism for Soot Formation in Nonpremixed Flames' *Comb & Flame* 87:289-305 (1991)
- Leung, K. M. (1996) PhD Thesis, Imperial College, London
- Magnussen, B. F. and Hjertager, B. H. (1976), 16th Symposium (International) on Combustion, pp 719
- Moss, J. B., Stewart, C. D. & Syed, K. J. (1988) 22nd Symposium (International) on Combustion, The Combustion Institute, pp 413-423

Nagle, J. And Strickland-Constable, R. F. (1962) Proc. 5th Carbon Conference, Vol. 1, pp 154
 Priddin, C. H. and Coupland, J. , 1988, "Impact of numerical methods on gas turbine design and development," Combustion, Science and Technology, Vol. 58, pp. 119

Sivathanu, Y.R & Gore J.P (1994), 'Coupled Radiation and Soot Kinetics Calculations in Laminar Acetylene/Air Diffusion Flames', Combustion and Flame 97:161-172 (1994)
 Tesner, P. A., Snegiriova, T. D. And Knorre, V. G. (1971), Combustion and Flame, Vol. 17, pp 253-26
 Young, K. J., Stewart, C. D. And Moss, J. B. (1991) Tenth ISABE Meeting, p 239-248

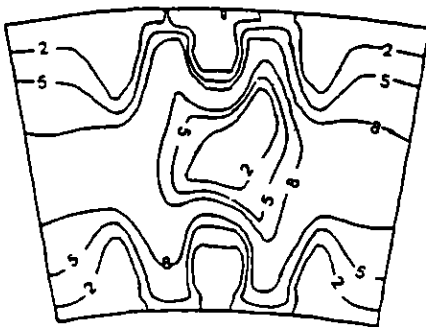


Predicted Primary Zone Exit

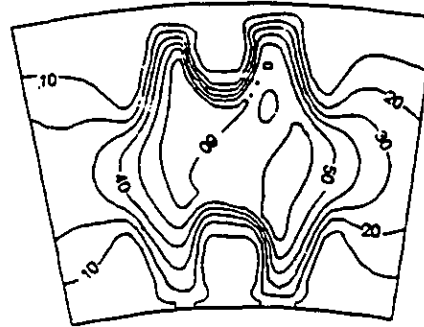


Predicted Combustor Exit

Figure 8 Soot Predicted by Lindstedt Model with Radiation in Gas Turbine Combustor (mg/m^3)



Moss Model (scaled by 1×10^{14})



Lindstedt Model (scaled by 1×10^{16})

Figure 9 Comparison of Number Densities Predicted in Gas Turbine Combustor

Downloaded from <http://asmelibrarycollection.asme.org/GT/proceedings-pdf/GT/1997/778699/V002T06A019/2409132/V00206A019-97-gt-148.pdf> by guest on 21 March 2025